Histochem Cell Biol (2002) 117:481–492
DOI 10.1007/s00418-002-0406-2

ORIGINAL PAPER

Jurgen Hens · Mariusz Gajda
Dietrich W. Scheuermann · Dirk Adriaensen
J.-P. Timmermans

The longitudinal smooth muscle layer of the pig small intestine is innervated by both myenteric and submucous neurons

Accepted: 21 March 2002 / Published online: 27 April 2002

Abstract Originally, intestinal motility was thought to be exclusively regulated by myenteric neurons. Some years ago, however, it was demonstrated in large mammals that submucous neurons also participate in the innervation of the circular smooth muscle layer. To date, no information is available about the submucous innervation of the longitudinal smooth muscle layer (LM). This study provides evidence that in the small intestine of large mammals, the LM is innervated not only by the myenteric plexus, but also by the inner and outer submucous plexuses (ISP and OSP). In the porcine small intestine, the involved neurons can be subdivided into the following neurochemically distinct populations: leu-enkephalin (ENK)- and/or substance P (SP)-IR neurons and nitric oxide synthase (NOS)- and/or vasoactive intestinal polypeptide (VIP)-IR neurons. In the myenteric plexus, the majority of VIP- and/or NOS-IR neurons and ENK^+/SP^--IR neurons exhibit descending projections, whereas ENK^+/SP^+-IR neurons preferentially have ascending projections. The ENK^-/SP^+-IR neurons do not show a polarized pattern. In the OSP, only ENK^+/SP^-- and VIP^+/NOS^--IR neurons display a polarized (descending) projection pattern, whereas no polarization can be noted in the ISP. Morphological analysis of the traced neurons revealed that, in general, myenteric descending LM motor neurons have larger cell bodies than ascending ones and, in addition, myenteric descending VIP- and/or NOS-IR neurons have longer projections than ENK and/or SP-IR neurons. In conclusion, the present study demonstrates the involvement of not only myenteric, but also submucous neurons in the innervation of the LM. The two major populations are descending nitrergic neurons and ascending tachykinergic motor neurons, but also other subpopulations with specific projection patterns and neurochemical features have been identified.

Keywords Enteric nervous system · DiI tracing · Spatial mapping · Neuropeptides · Organotypic culture

J. Hens · D.W. Scheuermann · D. Adriaensen
J.-P. Timmermans (✉)
Laboratory of Cell Biology and Histology, University of Antwerp, Groenenborgerlaan 171, 2020 Antwerp, Belgium
e-mail: jptimmer@ruca.ua.ac.be
Tel.: +32-3-2180300, Fax: +32-3-2180301

M. Gajda
Department of Histology, Jagiellonian University, Medical College, Kraków, Poland

Introduction

At the end of the nineteenth century, it was demonstrated that intraluminal distension of an extrinsically denervated intestinal segment evokes a contraction of the smooth muscle layer oral and a relaxation anal to the stimulus (Bayliss and Starling 1899). The debate whether this so-called "Law of the Intestine" still holds true and whether local physiological stimulation of the small intestine elicits synchronous contractions and relaxations of the longitudinal (LM) and circular (CM) smooth muscle layers has recently been revived. Original data of Kottegoda (1969) suggesting a reciprocal innervation of the CM and LM are challenged by a number of studies indicating that both muscle layers contract and relax together (McKirdy 1972; Smith and Robertson 1998; Spencer et al. 1999; Wood and Perkins 1970). A recent study has demonstrated that these synchronous contractions do not result from electrical coupling between the CM and LM, but are induced by separate populations of motor neurons to both muscle layers (Stevens et al. 2000).

Although the most widely studied preparation for investigating the pharmacology and physiology of neurotransmission to the intestinal smooth muscle in vitro is the longitudinal muscle–myenteric plexus (LMMP) preparation, most immunohistochemical studies dealing with the neurochemical coding of enteric motor neurons primarily focus on the CM. In most species, this muscle layer is much more pronounced and is more densely innervated than the LM.

Contraction and relaxation of both external smooth muscle layers are mainly mediated by neurons located in the myenteric plexus (MP). Combined use of neuronal

tracing, c-fos expression and immunohistochemistry, however, revealed submucous neurons in the guinea pig intestine projecting to the MP (Kirchgessner and Gershon 1988; Kirchgessner et al. 1992; Song et al. 1998). These studies have shown that in small mammals submucous neurons are not directly involved in the innervation of both external smooth muscle layers. However, in larger mammals such as dog, pig, and humans, intestinal neurons of the outer submucous plexus (OSP) were found to project to the CM, MP, and even to participate in viscerofugal pathways (Barbiers et al. 1994, 1995; Domoto et al. 1990; Sanders and Smith 1986; Timmermans et al. 1994a). To date, no data have been reported on the possible involvement of submucous neurons in the innervation of the LM. Given the necessity of coordinated CM and LM movements for adequate peristalsis (Spencer et al. 1999; Waterman and Costa 1994) as well as the demonstrated participation of the OSP in the innervation of the CM, it might be possible that the submucous plexuses also contribute to the innervation of the LM. As such, these nerve networks are ideally positioned to perform a coordinating and integrating function between mucosal and motility processes.

In view of the existing species differences, the aims of the present study were to pinpoint the exact location of enteric neurons innervating the LM of the porcine small intestine by applying a retrograde carbocyanine tracer to the LM, to analyze their neurochemical coding and to check whether submucous neurons are also involved in these pathways. In order to characterize the distinct subpopulations of inhibitory and excitatory LM motor neurons, antibodies raised against substance P (SP), leu-enkephalin (ENK), vasoactive intestinal polypeptide (VIP), and nitric oxide synthase (NOS) were used. Subsequently, the distribution of different classes of traced neurons between the distinct nerve networks was mapped and the oral–aboral polarized patterns of the assumed inhibitory and excitatory motor neurons were examined.

Materials and methods

Tissue collection and preparation

Ten 6-week-old domestic pigs were killed by cerebral trauma and exsanguination via the carotid arteries. The experiments were approved by the ethics committee of the University of Antwerp. Jejunal segments were removed and rinsed immediately with an oxygenated Krebs solution (95% CO_2, 5% O_2) containing 117.0 mM NaCl, 5.0 mM KCl, 2.5 mM $CaCl_2.2H_2O$, 1.2 mM $MgSO_4.7H_2O$, 25.0 mM $NaHCO_2$, 1.2 mM $NaH_2PO_4.2H_2O$, 10.0 mM glucose, and 1 µM nicardipine (4°C, pH 7.4). The specimens were cut open along the mesenteric border and agitated in fresh aerated Krebs solution to remove the intestinal content. The segments were then pinned out with the luminal side upward in a Sylgard-lined Petri dish containing oxygenated Krebs solution. Subsequently, the whole mounts were pinned with the abluminal side up and part of the serosa was removed to expose the LM. The tip of a micropipette, on which DiI (D-383; Molecular Probes Europe, Leiden, The Netherlands) was precipitated, was put on top of the LM using a micromanipulator. During this procedure, the tissue was continuously perfused by fresh Krebs solution (Hens et al. 2000). After 10 min, when the DiI tip was attached to the muscle, the specimens were transferred to a sterile Sylgard-lined Petri dish filled with Dulbecco's modified Eagle medium (DME/F12-HAM; Sigma Chemical, St. Louis, Mo., USA) containing 10 mg/ml antibiotic-antimycotic (Sigma), 50 µg/ml gentamicin (Sigma), 2.5 µg/ml amphotericin B (Sigma), 10% fetal bovine serum (Sigma), 1 µM nifedipine, and 2.1 mg/ml $NaHCO_3$, and incubated in a humidified CO_2 incubator for 3 days. Prolonging the incubation time did not result in an increased number of traced neurons. Petri dishes were agitated at a constant speed of 0.6–0.8 Hz to stabilize the pH of the medium underneath the whole mounts.

Preparations in which, prior to DiI application, the external longitudinal smooth muscle layer was disconnected from the rest of the gut wall and placed back in its original position, served as controls. In this way, the axons running from the muscle to the submucosa and vice versa were disrupted and the DiI molecules could not be transported specifically along the nerve fibers.

Immunohistochemistry

Following organotypic culturing, the tissues were fixed in Zamboni's fixative (15% saturated picric acid and 4% paraformaldehyde in 0.1 M phosphate buffer; pH 7.0) for 2 h at room temperature. After rinsing in 0.01 M phosphate-buffered saline (PBS) to remove the excess of fixative, two types of whole mounts were prepared, i.e., an LMMP preparation, and a preparation of the submucosa containing the inner submucous plexus (ISP) on the luminal side, consisting of small ganglia, and the OSP on the abluminal side, harboring larger ganglia. Antibody penetration was enhanced by incubating the tissues in $NaHCO_3/Na_2CO_3$ solutions (0.5 M; pH 8.6) containing different glycerol concentrations: 30 min in 50% glycerol, 30 min in 80% glycerol, and 120 min in 100% glycerol (Neunlist and Schemann 1997). Afterwards, the glycerol was removed by rinsing the tissues in PBS. To prevent non-specific binding of antibodies, the preparations were incubated for 30 min in 0.01 M PBS containing 10% normal goat serum, 0.1% bovine serum albumin, 0.05% thimerosal, and 0.01% NaN_3. The whole mounts were incubated in primary antisera (Table 1) for 48 h at room temperature. After six washes of 5 min in PBS, the preparations were incubated in secondary antisera (Table 1) for 6 h at room temperature. The tissues were rinsed again and incubated in streptavidin conjugated to 7-amino-4-methylcoumarin-3-acetic acid (Jackson Immunoresearch Laboratories, West Grove, Pa., USA) for an additional 6 h. After a final wash in PBS, the whole mounts were mounted in Vectashield and examined under an Olympus BX-50 fluorescence microscope. A Zeiss LSM-510 confocal microscope, equipped with a helium-neon laser (543 nm), an argon laser (488 nm), and a titanium:sapphire laser (tunable from 700 to 1,000 nm for two-photon excitation), was used to capture images of single or double immunolabeled retrograde traced cells.

Cell measuring, cell mapping, and statistical procedure

For quantitative analysis of the size of the cell bodies and spatial mapping of traced neurons, an Olympus BX-50 fluorescence microscope was equipped with a computerized stage mapping system and a CCD camera, which was coupled to a personal computer with Analysis Pro 3.00 software (Soft Imaging System, Münster, Germany). The area of the traced perikarya was measured and the mean percentages of DiI-labeled immunoreactive neurons relative to all traced neurons were calculated. Scatter plots of traced neurons were created with GraphPad Prism 5.02 (GraphPad Software, San Diego, Calif., USA). Statistical analysis of the differences in distribution of traced cells and the mean size of the cell bodies of distinct populations were examined with Graphpad Instat 3.05 (GraphPad Software) using an unpaired *t*-test (with or without Welch correction).

Table 1 List of antisera used for immunohistochemistry

Antigen	Host	Dilution	Source
Primary antisera			
Substance P (SP)	Rat	1:100	34HL; Biogenesis, Poole, UK
Vasoactive intestinal polypeptide (VIP)	Rabbit	1:400	VA1285; Affiniti
Nitric oxide synthase (NOS)	Mouse	1:500	N2280; Sigma, St Louis, Mo., USA
L-enkephalin (ENK)	Rabbit	1:100	EA1149; Affinity
Secondary antisera and streptavidin complex			
Biotinylated anti-mouse IgG	Sheep	1:100	RPN 1001; Amersham Life Science, Aylesbury, UK
Biotinylated anti-rat IgG	Sheep	1:100	RPN 1002; Amersham Life Science
Fluorescein isothiocyanate-conjugated anti-rabbit IgG	Goat	1:100	4050–02; Southern Biotechnology Associates, Birmingham, UK
Streptavidin-7-amino-4-methylcoumarin-3-acetic acid (AMCA)		1:100	016–150–084; Jackson Immunoresearch Laboratories, West Grove, Pa., USA

Results

Distribution of enteric neurons innervating the longitudinal smooth muscle layer

Application of DiI onto the serosal side of the LM resulted in a bright red spot in the external smooth muscle layers and a fainter spot in the submucosa. At the center of these diffusion spots, a few diffusely stained neuronal cell bodies could be detected, but this staining pattern clearly differed from the typical granular cytoplasmic staining of neuronal cell bodies whose nerve terminals had specifically taken up the dye at the nerve terminals. In order to avoid possible inclusion of neurons with targets other than the LM, the few diffusely stained cells within the diffusion spots were discarded from this study. In control preparations, where the LM was partially disconnected from the rest of the gut wall, a similar spot was visible in both parts of the specimen. These preparations disclosed, however, no traced neurons in the submucous layers, indicating that the DiI labeling of submucous neurons in normal preparations was not due to diffusion or unspecific uptake of the dye by axons or cell bodies. Antibodies against SP, ENK, VIP, and NOS allowed to neurochemically differentiate between functionally distinct traced neuron populations. No colocalization of ENK/NOS, VIP/SP, or SP/NOS could be demonstrated in the traced cell population. Since the antibodies against ENK and VIP were both raised in rabbits, no reliable double-staining experiments could be performed for these substances.

Myenteric plexus

The vast majority (86%) of the neurons traced from the LM were located in the MP. The total number of traced neurons per preparation within this plexus ranged from 22 to 145. These neurons could be subdivided into at least seven groups (Table 2). The two major populations were neurons expressing both SP- and ENK-IR (Fig. 1Q–T; 27%) and neurons exhibiting both VIP- and NOS-IR (Fig. 1A–D *arrowhead*; 37%). Next to these two populations, ENK^+/SP^-- (Fig. 1M–P; 12%), ENK^-/SP^+- (Fig. 1I–L; 8%), VIP^+/NOS^-- (Fig. 1A–D *arrow*; 9%), and VIP^-/NOS^+-IR (Fig. 1E–H; 2%) DiI-labeled neurons were observed as well. About 5% of the traced neurons could not be identified neurochemically by the above-mentioned substances.

Table 2 Percentage of DiI-labeled and neurochemically identified neurons traced from the longitudinal smooth muscle layer. Values represent mean percentages ±SD. Each percentage of the neurochemically identified neuron populations is based on 6 preparations per plexus, except for the percentage of DiI labeled neurons, which is based on 14 specimens per plexus. (*ISP* Inner submucous plexus, *OSP* outer submucous plexus, *MP* myenteric plexus)

	ISP	OSP	MP
ENK^+/SP^+	0	29±14	27±10
ENK^-/SP^+	0.5±0.4	3±2	8±5
ENK^+/SP^-	0	21±3	12±2
VIP^+/NOS^+	5±3	20±18	37±17
VIP^+/NOS^-	58±16	20±5	9±3
VIP^-/NOS^+	0	4±3	2±1
Unidentified	36.5	3	5
DiI-labeled	4±3	10±6	86±7

Scatter plots revealed a polarized pattern of these distinct populations of traced neurons (Fig. 2). The mean and maximum distances of axonal projections of each neurochemical population are listed in Table 3. In general, descending VIP- and/or NOS-IR neurons exhibit longer axonal projections than ENK- and/or SP-IR neurons ($p<0.05$).

Most of the ENK^+/SP^+-IR traced neurons were located aborally to the DiI application spot (Fig. 2C; $P<0.05$), whereas ENK^+/SP^--IR DiI-labeled cell bodies were all located at the oral side (Fig. 2A; $P<0.05$). The ENK^-/SP^+-IR traced neurons showed no obvious polarized pattern (Fig. 2B).

The vast majority of VIP^+/NOS^+-, VIP^+/NOS^--, and VIP^-/NOS^+-IR traced neurons were found at the oral side of the DiI application spot (Fig. 2D–F; $P<0.05$). Part of these neurons, however, could also be traced aborally to the application spot.

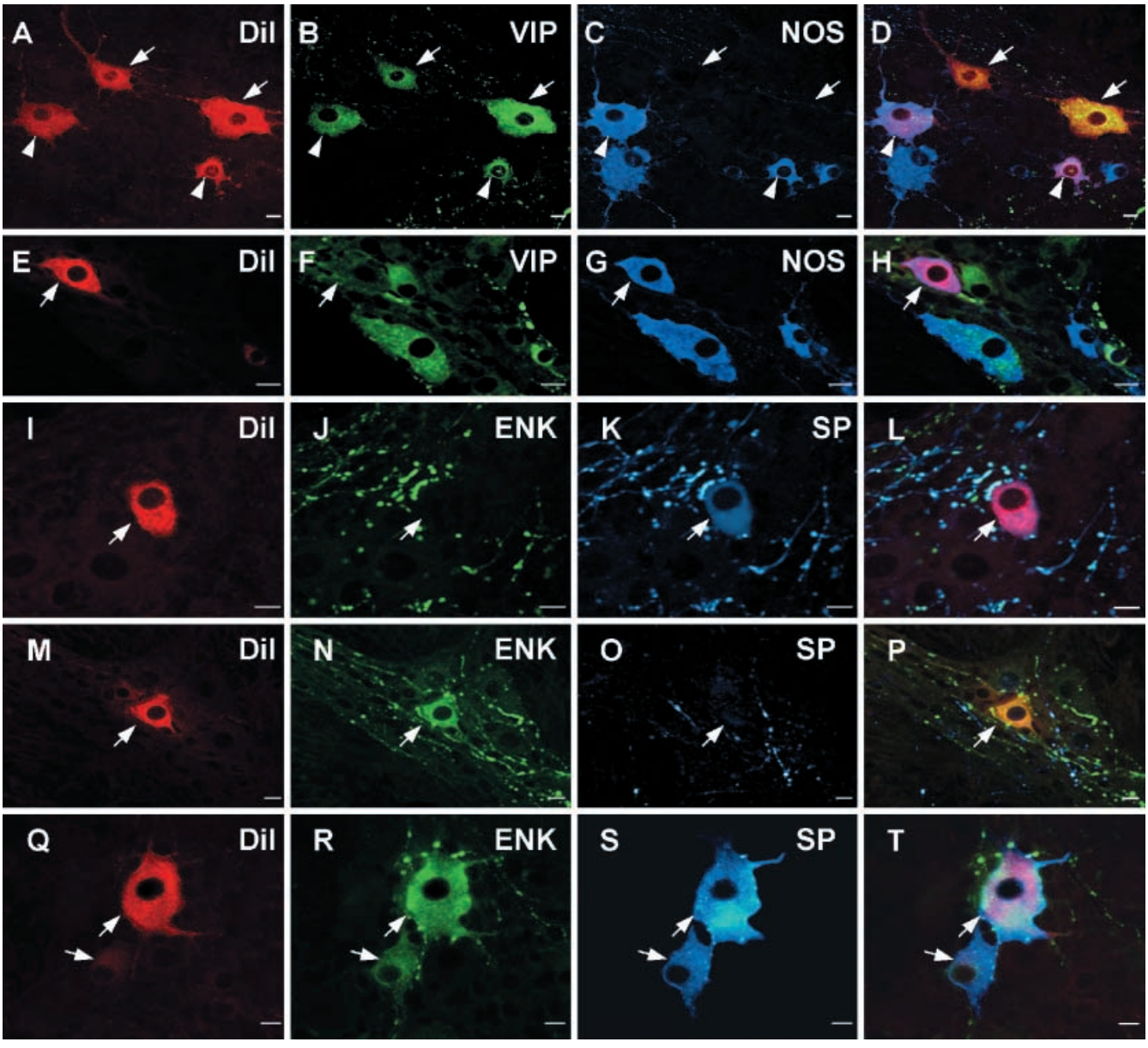

Fig. 1A–T Confocal (*red* and *green*) and two-photon (*blue*) images of myenteric neurons traced from the longitudinal smooth muscle layer (LM) of the pig small intestine. **A–D** Traced neurons expressing VIP$^+$/NOS$^-$-IR (*arrows*) and traced neurons expressing VIP$^+$/NOS$^+$-IR (*arrowheads*). **E–H** A traced neuron immunoreactive for VIP$^-$/NOS$^+$ (*arrows*). **I–L** A neuron exhibiting ENK$^-$/SP$^+$-IR. In **M–P**, an ENK$^+$/SP$^-$-IR neuron is shown (*arrows*) and ENK$^+$/SP$^+$-IR neurons are illustrated in **Q–T**. *Scale bars* 10 µm

Quantification of the size of each of the traced cell bodies revealed some striking differences (Table 4). The ENK$^+$/SP$^-$-IR neurons (mean=891 µm^2) had significantly larger cell bodies than ENK$^-$/SP$^+$-IR neurons (mean=403 µm^2; P<0.0001) and ENK$^+$/SP$^+$-IR neurons (mean=491 µm^2; P<0.0001). The latter cell bodies were significantly larger than ENK$^-$/SP$^+$-IR neurons (P<0.0001). The size of traced VIP$^+$/NOS$^-$-IR cell bodies (mean=1,214 µm^2) was significantly larger compared to that of VIP$^+$/NOS$^+$-IR (mean=935 µm^2; P<0.0001) and VIP$^-$/NOS$^+$-IR cell bodies (mean=339 µm^2; P<0.0001). The latter neurons had significantly smaller cell bodies than VIP$^+$/NOS$^+$-IR neurons (P<0.0001).

Outer submucous plexus

The OSP harbored 10% of all neurons traced from the LM. The total number of traced neurons per preparation within this plexus ranged from 3 to 16. As in the MP, seven neurochemically different subpopulations could be identified (Table 2). In contrast to the MP, ENK$^+$/SP$^+$- (Fig. 3E–H *arrowhead*; 29%) and VIP$^+$/NOS$^+$-IR (Fig. 3M–P *arrow*; 20%) neurons did not represent the only major populations of traced cells since the ENK$^+$/SP$^-$- (Fig. 3E–H *arrow*; 21%) and VIP$^+$/NOS$^-$-IR

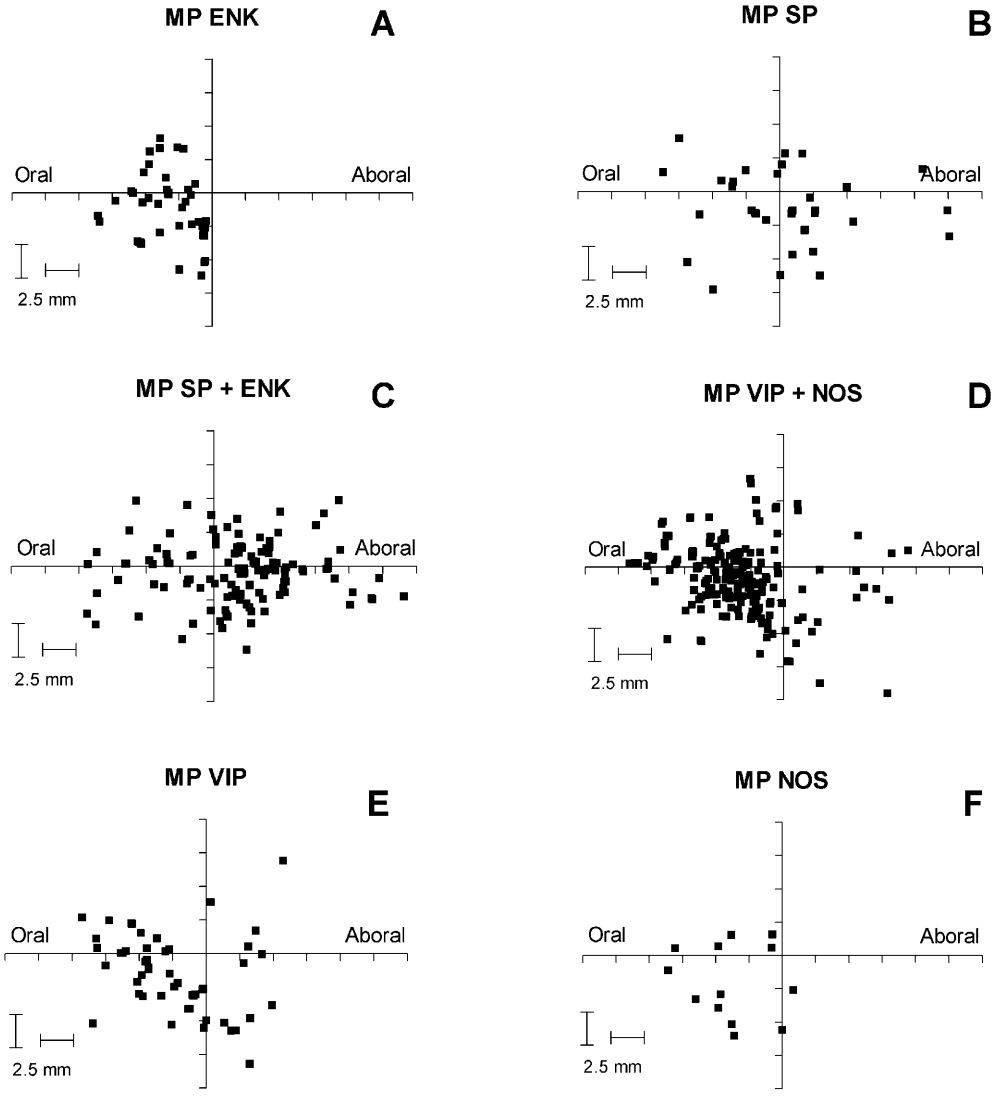

Fig. 2 Scatter plots of traced neurons in the myenteric plexus (MP) of the pig small intestine, immunoreactive for ENK (**A**), SP (**B**), SP and ENK (**C**), VIP and NOS (**D**), VIP (**E**), and NOS (**F**). The *center of the graphs* corresponds to the DiI application spot and each *point* represents one traced neurochemically identified neuron. Virtually all ENK$^+$/SP$^-$-IR neurons are located at the oral side of the DiI application spot (**A**), ENK$^-$/SP$^+$-IR neurons have no obvious polarized pattern (**B**), ENK$^+$/SP$^+$-IR neurons are preferentially located at the aboral side (**C**), and the majority of VIP- and/or NOS-IR neurons are situated at the oral side (**D–F**)

Table 3 Mean and maximum distances between traced nerve cell bodies and site of tracer application. (*ND* Not detected)

	ISP				OSP				MP			
	Oral (µm)		Aboral (µm)		Oral (µm)		Aboral (µm)		Oral (µm)		Aboral (µm)	
	Mean	Max	Mean	Max	Mean	Max	Mean	Max	Mean	Max	Mean	Max
ENK$^+$/SP$^+$	ND	ND	ND	ND	2,381	5,304	1,902	3,762	4,075	9,415	3,898	14,048
ENK$^-$/SP$^+$	ND	ND	3,294	3,294	3,412	5,916	ND	ND	3,909	8,684	3,418	12,556
ENK$^+$/SP$^-$	ND	ND	ND	ND	3,788	7,418	47	47	3,312	8,571	ND	ND
VIP$^+$/NOS$^+$	2,053	3,667	ND	ND	3,496	5,708	212	398	4,633	11,667	3,512	9,390
VIP$^+$/NOS$^-$	3,289	7,911	1,644	3,160	4,021	7,477	1,823	4,604	4,258	9,287	3,039	5,718
VIP$^-$/NOS$^+$	ND	ND	ND	ND	ND	ND	669	1,293	4,061	8,570	409	818

(Fig. 3I–L; 20%) populations appeared to be of comparable size. The ENK$^-$/SP$^+$- (Fig. 3A–D) and VIP$^-$/NOS$^+$-IR neurons (Fig. 3M–P *arrowhead*) accounted for merely 3% and 4% of the traced cells, respectively, and approximately 3% of the traced cells in this plexus could not be identified by the applied neurochemical markers.

In this plexus, both VIP$^+$/NOS$^-$-IR and ENK$^+$/SP$^-$-IR neurons were preferentially located at the oral side of the application spot, but no clear-cut polarized pattern could be detected for the other (ENK- and/or SP-IR or VIP- and/or NOS-IR) subpopulations (Fig. 4A, B). The mean and maximum distances of axonal projections of each

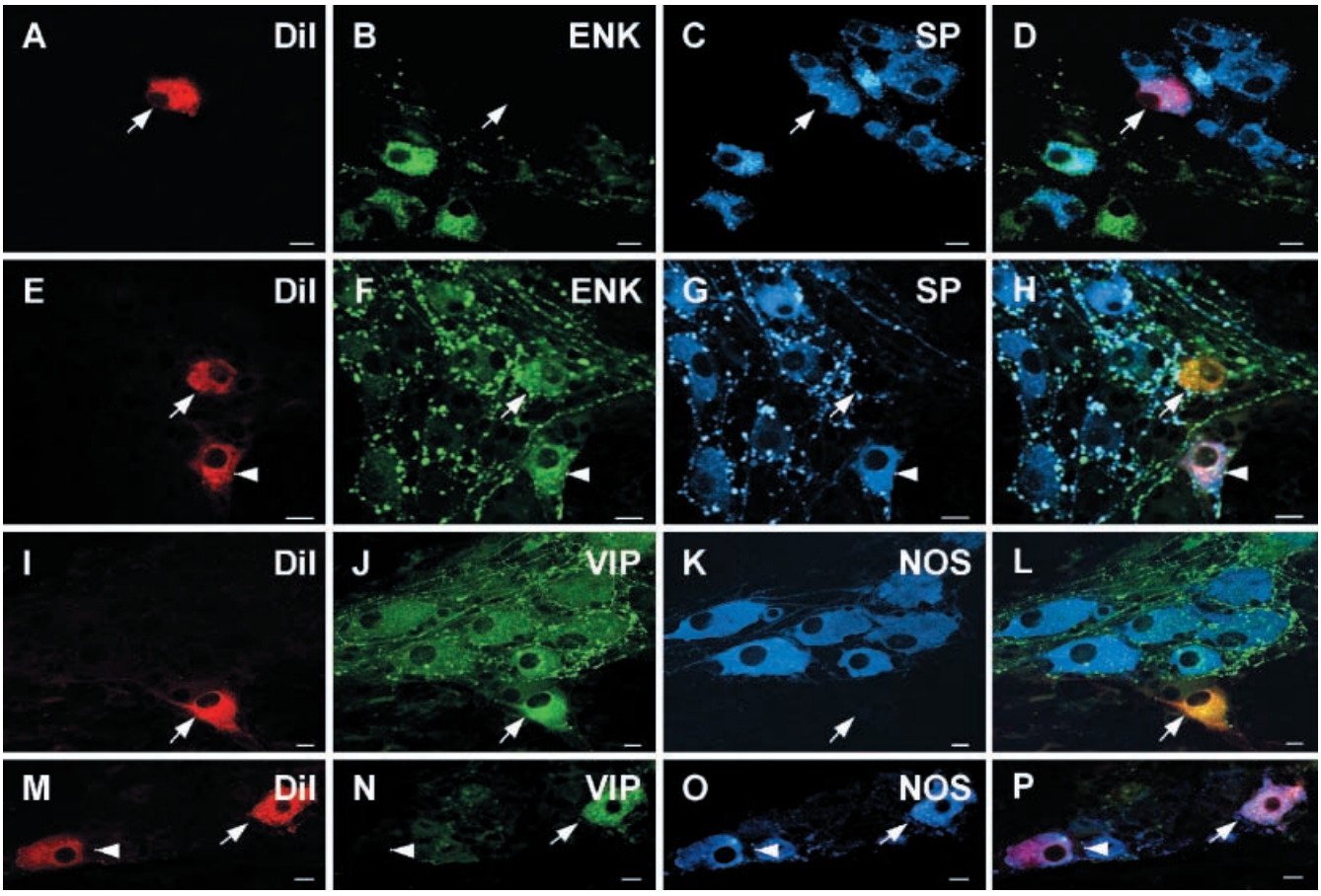

Fig. 3A–P Confocal (*red* and *green*) and two-photon (*blue*) images of outer submucous plexus (OSP) neurons traced from the LM of the pig small intestine. **A–D** A traced neuron which exhibits immunoreactivity for ENK$^-$/SP$^+$ (*arrows*). In **E–H**, a neuron expressing ENK$^+$/SP$^-$ (*arrows*) and an ENK$^+$/SP$^+$-IR neuron (*arrowheads*) are demonstrated. **I–L** A traced VIP$^+$/NOS$^-$-IR neuron (*arrows*). In **M–P** a VIP$^+$/NOS$^+$-IR neuron (*arrows*) and a VIP$^-$/NOS$^+$-IR neuron (*arrowheads*) are shown. *Scale bars* 10 µm

Table 4 Mean size of traced nerve cell bodies. Values represent mean size of traced cell bodies (µm^2) ±SD. (*NP* Not present; *ND* Not determined)

	ISP	OSP	MP
ENK$^+$/SP$^+$	NP	798±184 (*n*=22)	491±86 (*n*=50)
ENK$^-$/SP$^+$	ND	ND	403±79 (*n*=34)
ENK$^+$/SP$^-$	NP	949±271 (*n*=16)	891±212 (*n*=41)
VIP$^+$/NOS$^+$	ND	986±132 (*n*=14)	935±265 (*n*=55)
VIP$^+$/NOS$^-$	191±18 (*n*=21)	975±136 (*n*=15)	1,214±260 (*n*=45)
VIP$^-$/NOS$^+$	NP	ND	339±133 (*n*=14)

neurochemical population are listed in Table 3 showing that descending neurons generally project over longer distances than ascending neurons.

Data about the size of traced cell bodies are summarized in Table 4. The ENK$^+$/SP$^-$-IR neurons (mean= 949 µm^2) had significantly larger cell bodies than ENK$^+$/SP$^+$-IR neurons (mean=798 µm^2; P<0.05). The size of VIP$^+$/NOS$^-$-IR neuronal cell bodies (mean= 975 µm^2) did not differ significantly from that of VIP$^+$/NOS$^+$-IR cell bodies (mean=986 µm^2). The mean size of ENK$^-$/SP$^+$- and VIP$^-$/NOS$^+$-IR cell bodies could not be calculated unambiguously due to the limited number of traced neurons.

Inner submucous plexus

The ISP harbored 4% of the DiI-labeled neurons traced from the LM. The total number of traced neurons per preparation within this plexus ranged from 1 to 10. The only four distinct subpopulations classified so far in this plexus, could be distinguished on the basis of their neurochemical content (Table 2).

The major group of traced ISP neurons could be identified as VIP$^+$/NOS$^-$-IR neurons (Fig. 5A–D; 58%). The VIP$^+$/NOS$^+$-IR neurons accounted for 5% of the traced neurons in the ISP (Fig. 5E–H). Only a few neurons (<1%) were found to express ENK$^-$/SP$^+$-IR (not illustrated). The other populations observed in the MP and OSP (ENK$^+$/SP$^-$-, ENK$^+$/SP$^+$-, and VIP$^-$/NOS$^+$-IR neurons) were not found in the ISP and a relatively high number of neurons in this nerve network could not be identified neurochemically (36.5%) by these markers.

No significant polarized pattern could be observed in any of the traced subpopulations (Fig. 4C). The mean

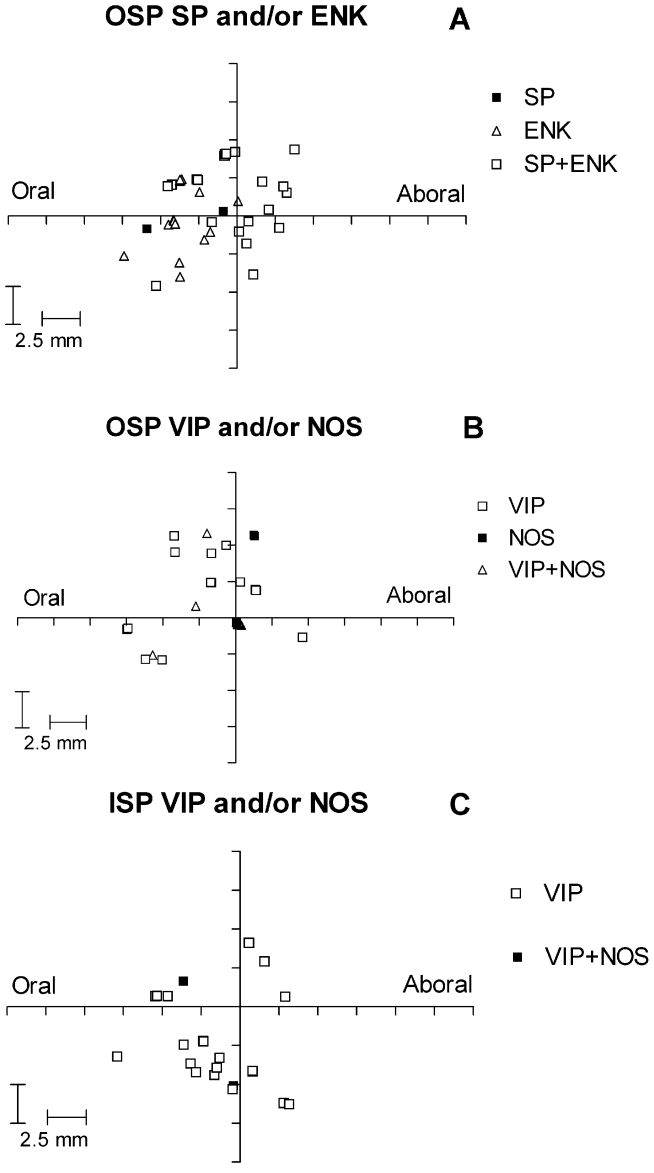

Fig. 4 Scatter plots of traced neurons in the OSP (**A**, **B**) and inner submucous plexus (ISP; **C**) of the pig small intestine, immunoreactive for SP and/or ENK (**A**) and VIP and/or NOS (**B**, **C**). The center of the graphs corresponds to the DiI application spot and each *point* represents one traced neurochemically identified neuron. In the OSP, both ENK$^+$/SP$^-$-IR neurons (**A**, *triangles*) and VIP$^+$/NOS$^-$-IR neurons (**B**, *open squares*) are preferentially located at the oral side of the DiI application spot. From the other cell populations in the OSP and ISP, no clear-cut polarized pattern can be deduced

and maximum distances of axonal projections of each neurochemical population are listed in Table 3.

The mean size of VIP$^+$/NOS$^-$-IR cell bodies in the ISP is 191 µm^2. Due to the limited number of traced cells, the mean size of VIP$^+$/NOS$^+$- and ENK$^-$/SP$^+$-IR cell bodies could not be calculated (Table 4).

Differences in cell body size between the three nerve networks

Comparison of the traced cell populations in the three nerve networks that expressed the same chemical coding yielded the following differences. Cell bodies in the ISP expressing VIP$^+$/NOS$^-$-IR were significantly smaller than those in the OSP (P<0.0001), which in turn were substantially smaller than those found in the MP (P<0.0001). The VIP$^+$/NOS$^+$-IR neuronal cell bodies in the OSP and MP showed comparable sizes. This also holds true for ENK$^+$/SP$^-$-IR neurons. In contrast, the size of ENK$^+$/SP$^+$-IR neuronal cell bodies was significantly larger in the OSP than that observed in the MP (P<0.0001).

Discussion

The present study provides for the first time evidence that apart from myenteric neurons submucous neurons are also involved in the innervation of the LM. In addition, a more detailed analysis of the neurochemical content of the distinct populations projecting to the LM has been achieved, indicating differences in the topographical distribution of these LM motor neuron populations (Fig. 6).

The majority of the motor neurons traced from the LM were found in the MP and could be subdivided into at least seven neurochemically different populations.

Substance P- and/or ENK-IR myenteric LM motor neurons

Compared to the guinea pig small intestine (Brookes et al. 1992), the proportion of myenteric SP-IR neurons projecting to the LM appears to be somewhat lower in the porcine small intestine (48% vs 35%). In the latter species, double labeling with ENK resulted in a further subdivision into three populations, two of which showing oppositely polarized distributions patterns. The majority of SP$^+$/ENK$^+$-IR LM motor neurons project orally, whereas the SP$^-$/ENK$^+$-IR cells send their axons in anal direction. Similar to the SP-IR LM motor neurons in the guinea pig small intestine (Brookes et al. 1992), the SP$^+$/ENK$^-$-IR LM motor neurons of the pig small intestine do not show a clear polarization of their axonal projections.

Specific polarized projection patterns of neurochemically identified enteric populations apparently are species- and region-dependent. A recent study demonstrating the presence of SP$^+$- and/or ENK$^+$-IR myenteric neurons innervating the LM of the guinea pig gastric corpus, revealed a projection pattern of the ENK$^+$/SP$^-$-IR subpopulation that was opposite to the one observed in the porcine small intestine (Michel et al. 2000). The SP$^+$/ENK$^+$-IR LM motor neurons, on the other hand, project mainly orally in both species and regions. The ENK$^-$/SP$^+$-IR LM motor neurons have orally directed projections in the guinea pig corpus, whereas in the

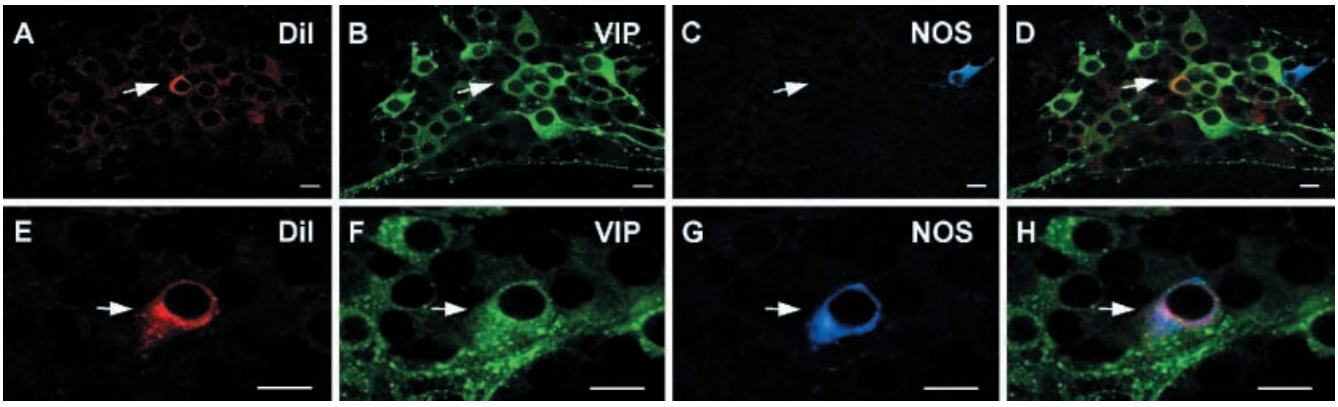

Fig. 5A–H Confocal (*red* and *green*) and two-photon (*blue*) images of ISP neurons traced from the LM of the pig small intestine. In **A–D**, a traced VIP$^+$/NOS$^-$-IR neuron is illustrated (*arrows*) and **E–H** demonstrates a VIP$^+$/NOS$^+$-IR neuron (*arrows*). *Scale bars* 10 µm

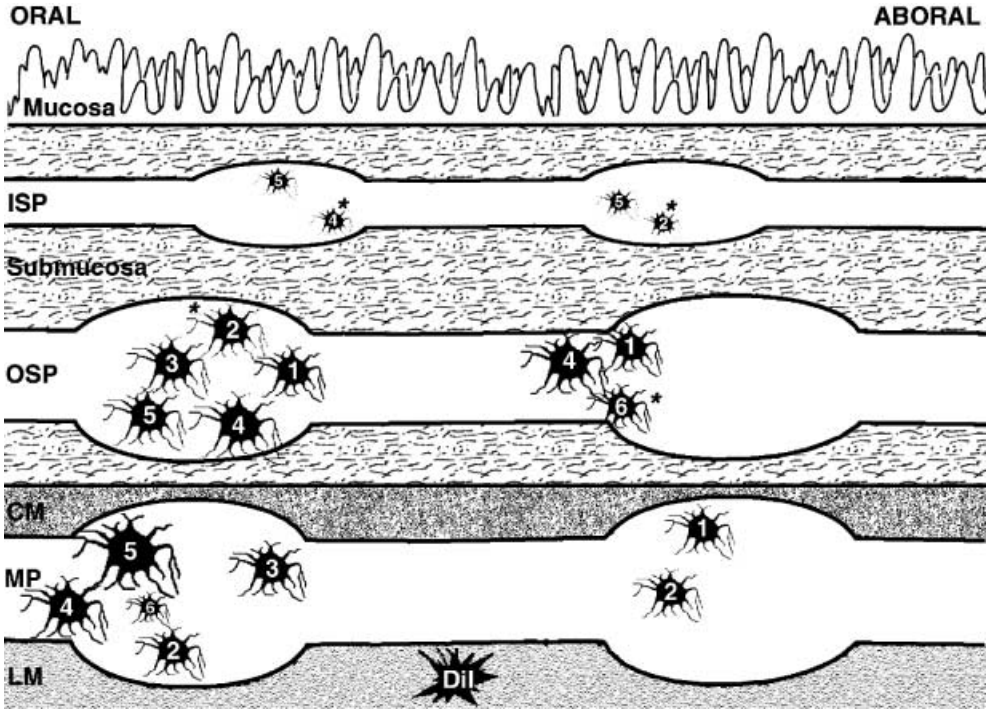

Fig. 6 Schematic overview of the distribution of LM motor neurons in the pig small intestine. Each cell represents its preferential localization oral or aboral to the DiI application spot related to the size of its cell body and mean projection distance. Cells that are depicted on both sides do not show an obvious polarization pattern. *ISP* Inner submucous plexus, *OSP* outer submucous plexus, *MP* myenteric plexus, *CM* circular smooth muscle, *LM* longitudinal smooth muscle, *DiI* DiI application spot, *1* ENK$^+$/SP$^+$, *2* ENK$^-$/SP$^+$, *3* ENK$^+$/SP$^-$, *4* VIP$^+$/NOS$^+$, *5* VIP$^+$/NOS$^-$, *6* VIP$^-$/NOS$^+$. *Asterisks* These cells could be demonstrated only on one side of the DiI application spot, but due to the limited number of these traced neurons, their polarization pattern could not be calculated statistically

guinea pig and pig small intestine they do not display a polarized projection pattern. To our knowledge, no data are available about the presence of ENK-IR LM motor neurons in the guinea pig small intestine, but some studies report the presence of varicose ENK-IR and SP-IR nerve fibers in the tertiary plexus and LM of the guinea pig colon (Messenger and Furness 1990). In addition, studies in the canine and feline ileum demonstrated SP- and ENK-IR varicose nerve fibers in the MP and both external smooth muscle layers (CM and LM; Bagnol et al. 1997; Daniel et al. 1987). Whether these SP-IR and ENK-IR nerve fibers in the LM show any coexistence is not clear at this moment, but colocalization of both substances is described in myenteric neuronal cell bodies of the cat and guinea pig ileum (Brookes et al. 1991a, 1997; Costa et al. 1996; Domoto et al. 1984). In the guinea pig small intestine, part of the ENK$^+$/SP$^+$-IR neurons are ascending excitatory motor neurons to the CM (Brookes et al. 1991b; Costa et al. 1996) and another part act as orally projecting interneurons (Brookes et al. 1997). Whether a third part of ENK$^+$/SP$^+$-IR neurons in the guinea pig are LM motor neurons needs further investigation. In this respect, it is also worth noting that ENK-IR CM motor neurons in the guinea pig small intestine that lack SP-IR, act as descending inhibitory motor neurons (Costa et al. 1996). This finding seems to be in accordance with our observation that virtually all ENK$^+$/SP$^-$-IR motor neurons projecting to the LM in both the MP and the OSP of the pig small intestine display descending axonal projections.

Apart from these morphological data, pharmacological studies have contributed greatly to unraveling the

possible functions of different neuropeptides. The tachykinin SP acts on neurokinin (NK) receptors that are present on mast cells (NK_1 receptors; Cooke et al. 1998; Okada et al. 1999), epithelial cells (NK_1 receptors; Southwell and Furness 2001), smooth muscle cells (NK_1 and NK_2 receptors), and enteric neurons (NK_1 and NK_3 receptors). In the small intestine of guinea pig, rat, dog, and human tachykinins have been described to exert a direct excitatory effect on the CM and LM by binding to NK_1 and/or NK_2 receptors (Bartho and Holzer 1985; Daniel et al. 1995; Holzer and Holzer-Petsche 1997a, b; Lordal and Hellstrom 1999; Zagorodnyuk et al. 1997).

There are some conflicting results about the physiological role of ENK in the digestive tract. Leu-enkephalin appears to be capable of exerting different actions on smooth muscle cells depending on the region of the gastrointestinal tract studied. In the rabbit, cat, and human colon, ENK inhibits non-adrenergic, non-cholinergic inhibitory neuromuscular transmission (Blanquet et al. 1982; Hoyle et al. 1990). In the rat ileum, on the other hand, ENK has been described to inhibit the ascending excitatory reflex response (Allescher et al. 2000). In addition, ENK has been demonstrated to act on the circular and longitudinal smooth muscle layers in a different way. In the feline duodenum, it contracts the LM and relaxes the CM, while in the feline jejunum it relaxes the LM and contracts the CM (Venkova et al. 1989). Due to these diverse functions and the lack of functional and pharmacological studies of ENK-containing neurons in the pig intestine, it is difficult to demonstrate the exact function of the traced ENK-IR neurons obtained in this study. The polarization results suggest that the majority of myenteric ENK-expressing neurons are ascending motor neurons. However, a substantial number of ENK-IR neurons, especially those lacking SP-IR, might be descending LM motor neurons. Whether these neurons can be classified as “ascending excitatory” and “descending inhibitory”, respectively, or whether part of these neurons are “descending excitatory” neurons (Hirst et al. 1975; Spencer et al. 1999) remains to be clarified by functional studies.

Vasoactive intestinal polypeptide- and/or NOS-IR myenteric LM motor neurons

A few decades ago, pharmacological evidence was found for the participation of NO (Boeckxstaens et al. 1991; Bult et al. 1990; Gibson et al. 1990; Gillespie et al. 1989; Hata et al. 1990) and VIP (Fahrenkrug et al. 1978; Goyal et al. 1980; Grider et al. 1985; Lefebvre et al. 1992) in the inhibitory neurotransmission in various organs, including the gastrointestinal tract. In addition, immunohistochemical studies identified enteric neurons that coexpress both substances in the rat gastrointestinal tract (Aimi et al. 1993), guinea pig small and large intestine (Costa et al. 1992; Lomax and Furness 2000), guinea pig stomach (Reiche and Schemann 1999), pig small and large intestine (Barbiers et al. 1994; Timmermans et al. 1994a), pig fundus (Lefebvre et al. 1995), and human small and large intestine (Keranen et al. 1995; Porter et al. 1999; Timmermans et al. 1994b). Recent experiments performed on synaptosomes that were isolated from rat small intestine, suggest an anatomical and functional interrelationship between NO and VIP and confirm the hypothesis of functional coupling between NO synthesis and VIP release (Kurjak et al. 2001).

With respect to the innervation of the LM in the pig small intestine, the present study has identified a fairly high number of VIP- and/or NOS-IR neurons (48% of all traced myenteric neurons). This finding contrasts with the situation in the guinea pig small intestine, which is characterized by a very small proportion of VIP-IR myenteric LM motor neurons (3%) and a paucity of VIP/NOS-IR varicose nerve fibers within this muscle layer (Brookes et al. 1992; Williamson et al. 1996). This suggests that virtually all motor neurons to the LM of the guinea pig small intestine are excitatory neurons. In the guinea pig colon and stomach, however, about 25% and 50% of LM motor neurons, respectively, modulate an inhibitory input to the muscle, illustrating once more the strong species and interregional differences of the enteric nervous system.

Projection distance and size of perikarya of myenteric LM motor neurons

In contrast to the guinea pig small and large intestine, where myenteric ascending and descending motor neurons innervating the LM are found in equivalent proportions (Brookes et al. 1992; Neunlist et al. 2001), but similar to the human small intestine (Wattchow et al. 1995), in pig, the population of descending LM motor neurons is larger than the ascending population.

The length of the axonal projections differs between the subpopulations. In general, descending VIP- and/or NOS-IR neurons project over longer distances than ENK- and/or SP-IR neurons.

The myenteric plexus of the pig small intestine reveals some striking differences in the size of the traced cell bodies of each neurochemical class. Apart from the VIP^-/NOS^+-IR cell population (which represents only 2% of the traced cells), it can be concluded that inhibitory LM motor neurons (descending) have larger cell bodies than excitatory ones (ascending) (mean= 1,013 μm^2 vs 447 μm^2). This observation is in agreement with the innervation of the CM seen in the guinea pig corpus (Brookes et al. 1998) and lower esophageal sphincter (Brookes et al. 1996). In the guinea pig small intestine and human small and large intestine, some data also point to this conclusion but quantitative evidence is still lacking (Brookes et al. 1991b; Wattchow et al. 1995, 1997). However, neither in the guinea pig nor in the human gastrointestinal tract have these differences in cell body size been described for LM motor neurons.

Submucous LM motor neurons

In the guinea pig small intestine, three types of submucous neurons have been described to project to the MP, i.e., SP-IR sensory neurons (Kirchgessner et al. 1992) and two types of interneurons (with and without VIP-IR) (Song et al. 1998). To our knowledge, no evidence for the existence of submucous neurons innervating the external smooth muscle layers is available in small laboratory animals (Song et al. 1998). The present study in the pig small intestine is hence the first reporting on submucous neurons that innervate the LM. Submucous neurons have been described earlier to innervate the CM in pig, dog, and human intestine (Porter et al. 1999; Sanders and Smith 1986; Timmermans et al. 1994a), but data on the LM are lacking in these large mammals. The present data suggest that part of the submucous neurons regulate the coordination between mucosal processes and motility. In small mammals, these submucous neurons might receive input from the mucosa and activate motor neurons in the MP, whereas in large mammals at least part of these submucous neurons might receive input from interneurons and act directly as motor neurons to the CM or LM.

Comparison of submucous LM motor neurons in the pig and submucous CM motor neurons in the human intestine reveals a similar distribution of the traced cells. In both species, only a minority of these neurons is located in the ISP (Porter et al. 1999). The majority is located in the OSP (pig and human) and intermediate submucous plexus (human). In both pig and human, a large part of the submucous motor neurons containing VIP-IR coexpress NOS-IR and do not show a polarized projection pattern. The VIP^+/NOS^-- and ENK^+/SP^--IR LM motor neurons are actually the only cells in the OSP of the pig small intestine that exhibit a polarized pattern. Remarkably, also in the MP, this is the only ENK- and/or SP-IR traced cell population that exhibits descending projections. Whether or not the same neurochemical classes of neurons traced from the LM in the ISP, OSP, and MP are functionally comparable remains to be investigated.

Conclusion

The present study clearly demonstrates that the three nerve networks present in the intestinal wall are involved in the innervation of the LM in the pig small intestine. In the MP and OSP, six classes of traced neurons could be identified neurochemically, whereas the ISP only harbored three types. The polarized pattern of the inhibitory and excitatory neurons is only significant in the MP. Interestingly, unlike ENK^+/SP^+- and ENK^-/SP^+-IR neurons, almost all ENK^+/SP^--IR LM motor neurons exhibit descending axonal projections in both the OSP and the MP.

Two major differences in the innervation of the LM were observed between guinea pig and pig small intestine. Firstly, in the guinea pig the LM innervation is restricted to the MP, while in the pig also the ISP and the OSP are involved. Secondly, in contrast to the pig, the majority of the LM motor neurons in the guinea pig are excitatory neurons.

To gain further insight into the communication between mucosal and motility processes, future research should be concentrated on mapping all cell populations involved and on identifying their anatomical interactions, which in turn would facilitate interpretation of physiological and pharmacological data.

Acknowledgements The authors would like to express their sincere thanks to F. Terloo, G. Govaerts, D. De Rijck, D. Vindevogel, and J. Van Daele for their excellent technical assistance. This investigation was supported by an IUAP grant (P4/16) of the Flemish Government and grants of the University of Antwerp (GOA 99/2/33 and RAFO).

References

Aimi Y, Kimura H, Kinoshita T, Minami Y, Fujimura M, Vincent SR (1993) Histochemical localization of nitric oxide synthase in rat enteric nervous system. Neuroscience 53:553–560

Allescher HD, Storr M, Brechmann C, Hahn A, Schusdziarra V (2000) Modulatory effect of endogenous and exogenous opioids on the excitatory reflex pathway of the rat ileum. Neuropeptides 34:62–68

Bagnol D, Henry M, Cupo A, Jule Y (1997) Distribution of enkephalin-like immunoreactivity in the cat digestive tract. J Auton Nerv Syst 64:1–11

Barbiers M, Timmermans JP, Scheuermann DW, Adriaensen D, Mayer B, De Groodt-Lasseel MHA (1994) Nitric oxide synthase-containing neurons in the pig large intestine: topography, morphology and viscerofugal projections. Microsc Res Tech 29:72–78

Barbiers M, Timmermans JP, Adriaensen D, Degroodtlasseel MHA, Scheuermann DW (1995) Projections of neurochemically specified neurons in the porcine colon. Histochem Cell Biol 103:115–126

Bartho L, Holzer P (1985) Search for a physiological role of substance P in gastrointestinal motility. Neuroscience 16:1–32

Bayliss WM, Starling EH (1899) The movements and innervation of the small intestine. J Physiol 24:99–143

Blanquet F, Bouvier M, Gonella J (1982) Effects of enkephalins and morphine on spontaneous electrical activity and on junction potentials elicited by parasympathetic nerve stimulation in cat and rabbit colon. Br J Pharmacol 77:419–429

Boeckxstaens GE, Pelckmans PA, Bogers JJ, Bult H, De Man JG, Oosterbosch L, Herman AG, Van Maercke YM (1991) Release of nitric oxide upon stimulation of nonadrenergic noncholinergic nerves in the rat gastric fundus. J Pharmacol Exp Ther 256:441–447

Brookes SJH, Steele PA, Costa M (1991a) Calretinin immunoreactivity in cholinergic motor neurones, interneurones and vasomotor neurones in the guinea-pig small intestine. Cell Tissue Res 263:471–481

Brookes SJH, Steele PA, Costa M (1991b) Identification and immunohistochemistry of cholinergic and non-cholinergic circular muscle motor neurons in the guinea-pig small intestine. Neuroscience 42:863–878

Brookes SJH, Song ZM, Steele PA, Costa M (1992) Identification of motor neurons to the longitudinal muscle of the guinea pig ileum. Gastroenterology 103:961–973

Brookes SJH, Chen BN, Hodgson WM, Costa M (1996) Characterization of excitatory and inhibitory motor neurons to the guinea pig lower esophageal sphincter. Gastroenterology 111:108–117

Brookes SH, Meedeniya AB, Jobling P, Costa M (1997) Orally projecting interneurones in the guinea-pig small intestine. J Physiol 505:473–491

Brookes SJH, Hennig G, Schemann M (1998) Identification of motor neurons to the circular muscle of the guinea pig gastric corpus. J Comp Neurol 397:268–280

Bult H, Boeckxstaens GE, Pelckmans PA, Jordaens FH, Van Maercke YM, Herman AG (1990) Nitric oxide as an inhibitory non-adrenergic non-cholinergic neurotransmitter. Nature 345: 346–347

Cooke HJ, Fox P, Alferes L, Fox CC, Wolfe SA (1998) Presence of NK1 receptors on a mucosal-like mast cell line, RBL-2H3 cells. Can J Physiol Pharmacol 76:188–193

Costa M, Furness JB, Pompolo S, Brookes SJH, Bornstein JC, Bredt DS, Snyder SH (1992) Projections and chemical coding of neurons with immunoreactivity for nitric oxide synthase in the guinea-pig small intestine. Neurosci Lett 148:121–125

Costa M, Brookes SJH, Steele PA, Gibbins I, Burcher E, Kandiah CJ (1996) Neurochemical classification of myenteric neurons in the guinea-pig ileum. Neuroscience 75:949–967

Daniel EE, Furness JB, Costa, Belbeck L (1987) The projections of chemically identified nerve fibres in canine ileum. Cell Tissue Res 247:377–384

Daniel EE, Parrish MB, Watson EG, Fox-Threlkeld JET, Regoli D, Rainsford KD (1995) The tachykinin receptors inducing contractile responses of canine ileum circular muscle. Am J Physiol 268:G161–G170

Domoto T, Gonda T, Oki M, Yanaihara N (1984) Coexistence of substance P- and methionine5-enkephalin-like immunoreactivity in nerve cells of the myenteric ganglia in the cat ileum. Neurosci Lett 47:9–13

Domoto T, Bishop AE, Oki M, Polak JM (1990) An in vitro study of the projections of enteric vasoactive intestinal polypeptide-immunoreactive neurons in the human colon. Gastroenterology 98:819–827

Fahrenkrug J, Haglund U, Jodal M, Lundgren O, Olbe L, Schaffalitzky de Muckadell OB (1978) Nervous release of vasoactive intestinal polypeptide in the gastrointestinal tract of cats: possible physiological implications. J Physiol 284:291–305

Gibson A, Mirzazadeh S, Hobbs AJ, Moore PK (1990) L-NG-monomethyl arginine and L-NG-nitro arginine inhibit non-adrenergic, non-cholinergic relaxation of the mouse anococcygeus muscle. Br J Pharmacol 99:602–606

Gillespie JS, Liu XR, Martin W (1989) The effects of L-arginine and NG-monomethyl L-arginine on the response of the rat anococcygeus muscle to NANC nerve stimulation. Br J Pharmacol 98:1080–1082

Goyal RK, Rattan S, Said SI (1980) VIP as a possible neurotransmitter of non-cholinergic non-adrenergic inhibitory neurones. Nature 288:378–380

Grider JR, Cable MB, Bitar KN, Said SI, Makhlouf GM (1985) Vasoactive intestinal peptide. Relaxant neurotransmitter in tenia coli of the guinea pig. Gastroenterology 89:36–42

Hata F, Ishii T, Kanada A, Yamano N, Kataoka T, Takeuchi T, Yagasaki O (1990) Essential role of nitric oxide in descending inhibition in the rat proximal colon. Biochem Biophys Res Commun 172:1400–1406

Hens J, Schrödl F, Brehmer A, Adriaensen D, Neuhuber W, Scheuermann DW, Schemann M, Timmermans J-P (2000) Mucosal projections of enteric neurons in the porcine small intestine. J Comp Neurol 421:429–436

Hirst GDS, Holman ME, McKirdy HC (1975) Two descending nerve pathways activated by distension of guinea-pig small intestine. J Physiol 244:113–127

Holzer P, Holzer-Petsche U (1997a) Tachykinins in the gut. 1. Expression, release and motor function. Pharmacol Ther 73:173–217

Holzer P, Holzer-Petsche U (1997b) Tachykinins in the gut. 2. Roles in neural excitation, secretion and inflammation. Pharmacol Ther 73:219–263

Hoyle CHV, Kamm MA, Burnstock G, Lennard-Jones JE (1990) Enkephalins modulate inhibitory neuromuscular transmission in circular muscle of human colon via delta-opioid receptors. J Physiol 431:465–478

Keranen U, Vanhatalo S, Kiviluoto T, Kivilaakso E, Soinila S (1995) Co-localization of NADPH diaphorase reactivity and vasoactive intestinal polypeptide in human colon. J Auton Nerv Syst 54:177–183

Kirchgessner AL, Gershon MD (1988) Projections of submucosal neurons to the myenteric plexus of the guinea pig intestine: in vitro tracing of microcircuits by retrograde and anterograde transport. J Comp Neurol 277:487–498

Kirchgessner AL, Tamir H, Gershon MD (1992) Identification and stimulation by serotonin of intrinsic sensory neurons of the submucosal plexus of the guinea pig gut: activity-induced expression of Fos immunoreactivity. J Neurosci 12: 235–248

Kottegoda SR (1969) An analysis of the possible nervous mechanisms involved in the peristaltic reflex. J Physiol 200:687–712

Kurjak M, Fritsch R, Saur D, Schusdziarra V, Allescher HD (2001) Functional coupling between nitric oxide synthesis and VIP release within enteric nerve terminals of the rat: involvement of protein kinase G and phosphodiesterase 5. J Physiol 534:827–836

Lefebvre RA, De Vriese A, Smits GJM (1992) Influence of vasoactive intestinal polypeptide and Ng-nitro-L-arginine methyl ester on cholinergic neurotransmission in the rat gastric fundus. Eur J Pharmacol 221:235–242

Lefebvre RA, Smits GJM, Timmermans JP (1995) Study of NO and VIP as non-adrenergic non-cholinergic neurotransmitters in the pig gastric fundus. Br J Pharmacol 116:2017–2026

Lomax AE, Furness JB (2000) Neurochemical classification of enteric neurons in the guinea-pig distal colon. Cell Tissue Res 302:59–72

Lordal M, Hellstrom PM (1999) The tachykinins neurokinin A and substance P, but not neurokinin B, stimulate contraction of isolated muscle cells from rat small intestine. Acta Physiol Scand 166:75–76

McKirdy HC (1972) Functional relationship of longitudinal and circular layers of the muscularis externa of the rabbit large intestine. J Physiol 227:839–853

Messenger JP, Furness JB (1990) Projections of chemically-specified neurons in the guinea-pig colon. Arch Histol Cytol 53:467–495

Michel K, Reiche D, Schemann N (2000) Projections and neurochemical coding of motor neurones to the circular and longitudinal muscle of the guinea pig gastric corpus. Pflugers Arch Eur J Physiol 440:393–408

Neunlist M, Schemann M (1997) Projections and neurochemical coding of myenteric neurons innervating the mucosa of the guinea pig proximal colon. Cell Tissue Res 287:119–125

Neunlist M, Michel K, Aubé A-C, Galmiche J-P, Schemann M (2001) Projections of excitatory and inhibitory motor neurones to the circular and longitudinal muscle of the guinea pig colon. Cell Tissue Res 305:325–330

Okada T, Hirayama Y, Kishi S, Miyayasu K, Hiroi J, Fujii T (1999) Functional neurokinin NK-1 receptor expression in rat peritoneal mast cells. Inflamm Res 48:274–279

Porter AJ, Wattchow DA, Brookes SH, Costa M (1999) Projections of nitric oxide synthase and vasoactive intestinal polypeptide-reactive submucosal neurons in the human colon. J Gastroenterol Hepatol 14:1180–1187

Reiche D, Schemann M (1999) Mucosa of the guinea pig gastric corpus is innervated by myenteric neurones with specific neurochemical coding and projection preferences. J Comp Neurol 410:489–502

Sanders KM, Smith TK (1986) Motoneurones of the submucous plexus regulate electrical activity of the circular muscle of canine proximal colon. J Physiol 380:293–310

Smith TK, Robertson WJ (1998) Synchronous movements of the longitudinal and circular muscle during peristalsis in the isolated guinea-pig distal colon. J Physiol 506:563–577

Song ZM, Costa M, Brookes SH (1998) Projections of submucous neurons to the myenteric plexus in the guinea pig small intestine. J Comp Neurol 399:255–268

Southwell BR, Furness JB (2001) Immunohistochemical demonstration of the NK1 tachykinin receptor on muscle and epithelia in guinea pig intestine. Gastroenterology 120:1140–1151

Spencer N, Walsh M, Smith TK (1999) Does the guinea-pig ileum obey the 'law of the intestine'? J Physiol 517:889–898

Stevens RJ, Publicover NG, Smith TK (2000) Propagation and neural regulation of calcium waves in longitudinal and circular muscle layers of guinea pig small intestine. Gastroenterology 118:892–904

Timmermans J-P, Barbiers M, Scheuermann DW, Stach W, Adriaensen D, Mayer B, De Groodt-Lasseel MHA (1994a) Distribution pattern, neurochemical features and projections of nitrergic neurons in the pig small intestine. Ann Anat 176:515–525

Timmermans JP, Barbiers M, Scheuermann DW, Bogers JJ, Adriaensen D, Fekete E, Mayer B, Vanmarck EA, Degroodtlasseel MHA (1994b) Nitric oxide synthase immunoreactivity in the enteric nervous system of the developing human digestive tract. Cell Tissue Res 275:235–245

Venkova K, Radomirov R, Pencheva N (1989) Effects of leuenkephalin on the mechanical activity of longitudinal and circular muscles of the small intestine of the cat. Neuropharmacology 28:1183–1191

Waterman SA, Costa M (1994) The role of enteric inhibitory motoneurons in peristalsis in the isolated guinea-pig small intestine. J Physiol 477:459–468

Wattchow DA, Brookes SJH, Costa M (1995) The morphology and projections of retrogradely labeled myenteric neurons in the human intestine. Gastroenterology 109:866–875

Wattchow DA, Porter AJ, Brookes SJH, Costa M (1997) The polarity of neurochemically defined myenteric neurons in the human colon. Gastroenterology 113:497–506

Williamson S, Pompolo S, Furness JB (1996) GABA and nitric oxide synthase immunoreactivities are colocalized in a subset of inhibitory motor neurons of the guinea-pig small intestine. Cell Tissue Res 284:29–37

Wood JD, Perkins WE (1970) Mechanical interaction between longitudinal and circular axes of the small intestine. Am J Physiol 218:762–768

Zagorodnyuk V, Santicioli P, Turini D, Maggi CA (1997) Tachykinin NK_1 and NK_2 receptors mediate non-adrenergic non-cholinergic excitatory neuromuscular transmission in the human ileum. Neuropeptides 31:265–271